

# NONLINEAR MAPPING OF GAUSSIAN STATE UNCERTAINTIES: THEORY AND APPLICATIONS TO SPACECRAFT CONTROL AND NAVIGATION

Ryan S. Park\* and Daniel J. Scheeres†

*The University of Michigan, Ann Arbor, MI 48109*

This paper discusses the nonlinear propagation of spacecraft trajectory uncertainties via solutions of the Fokker-Planck equation. We first discuss the solutions of the Fokker-Planck equation for a deterministic system with a Gaussian boundary condition. Next we derive an analytic expression of a nonlinear trajectory solution using a higher-order Taylor series approach, discuss the region of convergence for the solutions, and apply the result to spacecraft applications. Such applications consist of nonlinear propagation of the mean and covariance matrix, design of statistically correct trajectories, and nonlinear statistical targeting. The two-body and Hill three-body problems are chosen as examples and realistic initial uncertainty models are considered.

## Nomenclature

$\mathcal{B}_o, \mathcal{B}$	=	initial and current state phase volumes
$\mathbf{D}$	=	diffusion characteristic matrix
$E[\cdot]$	=	expectation operator
$\mathbf{f}$	=	system dynamics vector
$H$	=	Hamiltonian function
$\mathbf{I}$	=	identity matrix
$\mathbf{J}$	=	symplectic identity matrix
$\mathbf{m}^o, \mathbf{m}$	=	initial and current state mean vectors
$\mathbf{m}_r, \mathbf{m}_v$	=	position and velocity mean vectors
$\mathbf{P}^o, \mathbf{P}$	=	initial and current state covariance matrices
$p$	=	probability density function
$\mathbf{Q}$	=	diffusion matrix
$\mathbf{q}, \mathbf{p}$	=	generalized coordinate and momenta vectors
$\mathbf{r}, \mathbf{v}$	=	spacecraft position and velocity vectors
$t^o, t$	=	initial and current times
$\mathbf{x}^o, \mathbf{x}$	=	initial and current state vectors
$x, y$	=	horizontal and vertical position components
$\dot{x}, \dot{y}$	=	horizontal and vertical velocity components
$n$	=	dimension of the system (Hamiltonian system has dimension $2n$ )
$\beta$	=	$s$ -dimensional Brownian motion or Wiener process vector
$\theta$	=	true anomaly, deg
$\mu_E$	=	Europa gravitational constant, $3,201 \text{ km}^3/\text{s}^2$
$\mu_\oplus$	=	Earth gravitational constant, $398,600 \text{ km}^3/\text{s}^2$

\*Graduate Research Assistant, PhD Candidate, Department of Aerospace Engineering, The University of Michigan, Ann Arbor, Michigan, Member AIAA, sanghp@umich.edu.

†Associate Professor, Department of Aerospace Engineering, The University of Michigan, Ann Arbor, Michigan, Associate Fellow AIAA, Member AAS, scheeres@umich.edu.

$\nu$	=	nonlinearity index
$\Phi$	=	state transition tensors (if no subindexes, state transition matrix)
$\phi$	=	solution flow
$\phi_r, \phi_v$	=	position and velocity solution flows
$\chi$	=	joint characteristic function
$\psi$	=	inverse solution flow
$\omega_E$	=	rotational rate of the Jupiter-Europa Hill 3-body problem, $2.048 \times 10^{-5}$ rad/s

## Introduction

Present-day orbit uncertainty propagation usually chooses between linearized propagation models<sup>1-3</sup> or full nonlinear Monte-Carlo simulations.<sup>4</sup> The linear assumption simplifies the problem a great deal; however, the solution fails to characterize trajectory statistics when the system is in a highly unstable environment or when mapped over a long time period. On the other hand, Monte-Carlo simulations provide true trajectory statistics, but are computationally intensive and statistics are computed only for a specific epoch and its associated uncertainties. A different approach to orbit uncertainty propagation has also been discussed by Junkins *et al.*,<sup>5,6</sup> where the effect of the coordinate system on the propagated statistics is thoroughly analyzed; however, the propagation method was based on the linear assumption and the system nonlinearity was not incorporated in the mapping.

In this paper we explore an alternate way to analyze trajectory statistics by incorporating higher order Taylor series terms that describe localized nonlinear motion, and by solving for the higher order state solutions as functions of initial conditions, which we call the state transition tensors (STT). The theory is reasonably straightforward and can be adapted to many spacecraft applications that assume linear theory. Once the STTs are computed, an analytic expression of the neighboring trajectories can be obtained, and we discuss criterion for convergence of the series. Park and Scheeres<sup>7</sup> have shown that the statistics (mean and covariance matrix) computed using the STT-approach provide good agreement with Monte-Carlo simulations over reasonable time periods, and we provide more examples using the two-body and Hill 3-body problems. Moreover, we provide a detailed discussion on the theoretical insights of this approach by solving the Fokker-Planck equation for the orbit probability density function (pdf) for a deterministic system.

As applications of the STT-propagated statistics, we discuss the design of a statistically correct trajectory and its application to nonlinear statistical targeting. Given a trajectory with a certain initial uncertainty distribution, it is an inevitable fact that the mean trajectory will, depending on the system's nonlinearity, deviate from the reference (nominal) trajectory. For this reason we introduce the concept of a statistically correct trajectory by solving for the initial state where its statistical mean trajectory will hit the desired target state (e.g., the final state of a boundary value problem), not the nominal trajectory. This is a rather counter-intuitive approach since this implies that the initial state must be different from the solution of the deterministic boundary value problem; however, this should yield a more realistic and accurate trajectory design according to probability theory.

When mapping the initial uncertainties, it would be ideal consider Monte-Carlo simulations. However, Monte-Carlo method does not provide an analytic framework to analyze the dependency of the initial condition on the propagated true statistics and is impractical to model. The significance of the STT formulation is that it provides an analytic expression of the propagated true statistics, and thus the problem of statistically correct trajectories can be solved via an iterative process. As the higher order STTs are considered (i.e., order of the Taylor series), the propagated uncertainties become essentially the same as the Monte-Carlo solutions, and thus provide a more realistic estimate of the state than the conventional linear method. As an extension of the statistically correct trajectory, we discuss the nonlinear statistical targeting method where we solve for a correction maneuver based on the true (statistical) trajectory. The usual linear targeting method solves for a maneuver of a deterministic trajectory, and hence, the final target will be slightly offset from the desired target and additional maneuvers are may be needed. If we solve for a correction maneuver using the STT-approach the number maneuvers may be reduced since it captures the system's nonlinearity and provides the most realistic trajectory for the given state uncertainties at

the time of maneuver. We derive necessary conditions required for this problem and present examples to better explain the difference between the linear and nonlinear methods.

## Nonlinear Mapping of the System Dynamics

Consider the spacecraft dynamics governed by the equations of motion as a function of the initial conditions, written in tensor notation:

$$\dot{\mathbf{x}}_i(t) = \mathbf{f}_i(t, \mathbf{x}(t)), \quad (1)$$

where  $\mathbf{x} = \{\mathbf{x}_i \mid i = 1, \dots, n\}$  and initial conditions  $\mathbf{x}_i(t^o) = \mathbf{x}_i^o$ . For a given initial condition, we denote the solution flow as

$$\mathbf{x}(t) = \phi(t; \mathbf{x}^o, t^o), \quad (2)$$

which is the mapping of the state at epoch to the state at a future time. The solution flow satisfies

$$\begin{aligned} \frac{d\phi}{dt} &= \mathbf{f}(t, \phi(t; \mathbf{x}^o, t^o)), \\ \phi(t^o; \mathbf{x}^o, t^o) &= \mathbf{x}(t^o). \end{aligned} \quad (3)$$

This is somewhat an obvious statement; however, this notation is convenient when we consider the flow of a region in phase space. Suppose we are given an initial phase volume,  $\mathcal{B}_o$ . The evolution of this phase volume can be stated as

$$\mathcal{B}(t) = \{\mathbf{x}(t) \mid \mathbf{x}(t) = \phi(t; \mathbf{x}^o, t^o) \forall \mathbf{x}^o \in \mathcal{B}_o\}. \quad (5)$$

Applying a similar approach the inverse solution flow can be stated as

$$\mathbf{x}^o = \phi(t^o; \mathbf{x}, t), \quad (6)$$

which leads to the identity

$$\mathbf{x}^o = \phi(t^o; \phi(t; \mathbf{x}^o, t^o), t). \quad (7)$$

To distinguish between the direct and inverse solution flows, we use the following notation for the inverse solution flow:

$$\mathbf{x}^o = \psi(t, \mathbf{x}; t^o), \quad (8)$$

which is an integral of motion of the system, and hence,  $d\mathbf{x}^o/dt = 0$ . These notations will be used later to solve the Fokker-Planck equations and to derive the nonlinear representations of the mean and covariance matrix.

Using the summation convention and applying a Taylor series expansion to the solutions, deviations from the nominal solution  $\delta\mathbf{x}_i(t) = \mathbf{x}_i(t) - \mathbf{x}_i^*(t)$  to the  $m^{\text{th}}$  order and its time derivatives can be represented as

$$\delta\mathbf{x}_i(t) = \sum_{p=1}^m \frac{1}{p!} \Phi_{i, k_1 \dots k_p} \delta\mathbf{x}_{k_1}^o \dots \delta\mathbf{x}_{k_p}^o, \quad (9)$$

$$\delta\dot{\mathbf{x}}_i(t) = \sum_{p=1}^m \frac{1}{p!} \mathbf{f}_{i, k_1 \dots k_p}^* \delta\mathbf{x}_{k_1} \dots \delta\mathbf{x}_{k_p}, \quad (10)$$

where  $k_j \in \{1, \dots, n\}$ , subscripts  $k_j$  denote the  $k_j^{\text{th}}$  component of the state vector,

$$\Phi_{i, k_1 \dots k_p} = \frac{\partial^p \mathbf{x}_i}{\partial \mathbf{x}_{k_1}^o \dots \partial \mathbf{x}_{k_p}^o}, \quad (11)$$

$$\mathbf{f}_{i, k_1 \dots k_p}^* = \left. \frac{\partial^p \mathbf{f}_i}{\partial \mathbf{x}_{k_1} \dots \partial \mathbf{x}_{k_p}} \right|_{\mathbf{x}=\mathbf{x}^*}, \quad (12)$$

and the superscript ‘\*’ represent the values computed along a reference (nominal) solution. As an example, the summation convention applied to the second order effect can be written for  $p = 2$  as:

$$\frac{1}{2}\Phi_{i,k_1k_2}\delta\mathbf{x}_{k_1}^o\delta\mathbf{x}_{k_2}^o = \sum_{k_1=1}^n\sum_{k_2=1}^n\frac{1}{2}\Phi_{i,k_1k_2}\delta\mathbf{x}_{k_1}^o\delta\mathbf{x}_{k_2}^o. \quad (13)$$

From now on, we will call the higher order partials of the state  $\mathbf{x}_i$  (i.e.,  $\Phi_{i,k_1\dots k_p}$ ) the State Transition Tensors (STT). These relate deviations in the initial conditions to deviations in the state at some future time. The time derivative of the deviation  $\delta\dot{\mathbf{x}}_i$  can also be obtained by differentiating Eqn. (9),

$$\delta\dot{\mathbf{x}}_i(t) = \sum_{p=1}^m\frac{1}{p!}\dot{\Phi}_{i,k_1\dots k_p}\delta\mathbf{x}_{k_1}^o\dots\delta\mathbf{x}_{k_p}^o \quad (14)$$

since only the STTs depend on time. In conventional practice researchers usually work with the case  $m = 1$  (i.e., first-order or linear analysis) where Eqns. (11) and (12) are simply the usual “state transition matrix” and the “linear dynamics matrix”, respectively. We later show that when the nonlinearity is strong, including higher order effects provides superior results as compared to conventional linear analysis.

Now, in order to analyze the deviation of  $\delta\mathbf{x}$  as an analytic function of the initial deviations, we must solve for the STTs. To obtain differential equations for the STTs, first substituting Eqn. (9) into Eqn. (10), which gives the equation of  $\delta\dot{\mathbf{x}}_i$  as a function of the STTs and initial conditions. By equating this with Eqn. (14) and balancing terms of the same order in  $\delta\mathbf{x}^o$ , we obtain the differential equations for the STTs ( $\dot{\Phi}_{i,k_1\dots k_n}$ ), where the ODE’s up to fifth order deviation are given in Eqns. (15-19).

$$\dot{\Phi}_{i,a} = \mathbf{f}_{i,\alpha}^*\Phi_{\alpha,a}, \quad (15)$$

$$\dot{\Phi}_{i,ab} = \mathbf{f}_{i,\alpha}^*\Phi_{\alpha,ab} + \mathbf{f}_{i,\alpha\beta}^*\Phi_{\alpha,a}\Phi_{\beta,b}, \quad (16)$$

$$\dot{\Phi}_{i,abc} = \mathbf{f}_{i,\alpha}^*\Phi_{\alpha,abc} + \frac{3}{2}\mathbf{f}_{i,\alpha\beta}^*\Phi_{\alpha,a}\Phi_{\beta,bc} + \frac{3}{2}\mathbf{f}_{i,\alpha\beta}^*\Phi_{\alpha,ab}\Phi_{\beta,c} + \mathbf{f}_{i,\alpha\beta\gamma}^*\Phi_{\alpha,a}\Phi_{\beta,b}\Phi_{\gamma,c}, \quad (17)$$

$$\begin{aligned} \dot{\Phi}_{i,abcd} &= \mathbf{f}_{i,\alpha}^*\Phi_{\alpha,abcd} \\ &+ 2\mathbf{f}_{i,\alpha\beta}^*\Phi_{\alpha,a}\Phi_{\beta,bcd} + 2\mathbf{f}_{i,\alpha\beta}^*\Phi_{\alpha,abc}\Phi_{\beta,d} + 3\mathbf{f}_{i,\alpha\beta}^*\Phi_{\alpha,ab}\Phi_{\beta,cd} \\ &+ 2\mathbf{f}_{i,\alpha\beta\gamma}^*\Phi_{\alpha,a}\Phi_{\beta,b}\Phi_{\gamma,cd} + 2\mathbf{f}_{i,\alpha\beta\gamma}^*\Phi_{\alpha,a}\Phi_{\beta,bc}\Phi_{\gamma,d} + 2\mathbf{f}_{i,\alpha\beta\gamma}^*\Phi_{\alpha,ab}\Phi_{\beta,bc}\Phi_{\gamma,d} \\ &+ \mathbf{f}_{i,\alpha\beta\gamma\delta}^*\Phi_{\alpha,a}\Phi_{\beta,b}\Phi_{\gamma,c}\Phi_{\delta,d}, \end{aligned} \quad (18)$$

$$\begin{aligned} \dot{\Phi}_{i,abcde} &= \mathbf{f}_{i,\alpha}^*\Phi_{\alpha,abcde} \\ &+ \frac{5}{2}\mathbf{f}_{i,\alpha\beta}^*\Phi_{\alpha,a}\Phi_{\beta,bcde} + \frac{5}{2}\mathbf{f}_{i,\alpha\beta}^*\Phi_{\alpha,abcd}\Phi_{\beta,e} + 5\mathbf{f}_{i,\alpha\beta}^*\Phi_{\alpha,ab}\Phi_{\beta,cde} + 5\mathbf{f}_{i,\alpha\beta}^*\Phi_{\alpha,abc}\Phi_{\beta,de} \\ &+ \frac{10}{3}\mathbf{f}_{i,\alpha\beta\gamma}^*\Phi_{\alpha,a}\Phi_{\beta,b}\Phi_{\gamma,cde} + \frac{10}{3}\mathbf{f}_{i,\alpha\beta\gamma}^*\Phi_{\alpha,a}\Phi_{\beta,bcd}\Phi_{\gamma,e} + \frac{10}{3}\mathbf{f}_{i,\alpha\beta\gamma}^*\Phi_{\alpha,abc}\Phi_{\beta,d}\Phi_{\gamma,e} \\ &+ 5\mathbf{f}_{i,\alpha\beta\gamma}^*\Phi_{\alpha,a}\Phi_{\beta,bc}\Phi_{\gamma,de} + 5\mathbf{f}_{i,\alpha\beta\gamma}^*\Phi_{\alpha,ab}\Phi_{\beta,bc}\Phi_{\gamma,de} + 5\mathbf{f}_{i,\alpha\beta\gamma}^*\Phi_{\alpha,ab}\Phi_{\beta,bc}\Phi_{\gamma,de} \\ &+ \frac{5}{2}\mathbf{f}_{i,\alpha\beta\gamma\delta}^*\Phi_{\alpha,a}\Phi_{\beta,b}\Phi_{\gamma,c}\Phi_{\delta,de} + \frac{5}{2}\mathbf{f}_{i,\alpha\beta\gamma\delta}^*\Phi_{\alpha,a}\Phi_{\beta,b}\Phi_{\gamma,cd}\Phi_{\delta,e} \\ &+ \frac{5}{2}\mathbf{f}_{i,\alpha\beta\gamma\delta}^*\Phi_{\alpha,a}\Phi_{\beta,bc}\Phi_{\gamma,d}\Phi_{\delta,e} + \frac{5}{2}\mathbf{f}_{i,\alpha\beta\gamma\delta}^*\Phi_{\alpha,ab}\Phi_{\beta,bc}\Phi_{\gamma,d}\Phi_{\delta,e} \\ &+ \mathbf{f}_{i,\alpha\beta\gamma\delta\epsilon}^*\Phi_{\alpha,a}\Phi_{\beta,b}\Phi_{\gamma,c}\Phi_{\delta,d}\Phi_{\epsilon,e}. \end{aligned} \quad (19)$$

The initial conditions for these STTs are simple,  $\Phi_{i,a}^o = 1$  if  $i = a$  and all other initial STTs are initially zero. After solving for the STTs, the higher order solutions can be computed by adding the deviations to the reference solution, or  $\mathbf{x}_i(t) = \mathbf{x}_i^*(t) + \delta\mathbf{x}_i(t)$ . Since the reference solutions  $\mathbf{x}_i^*(t)$  are solved while computing the STTs,  $\mathbf{x}_i(t)$  can now be computed as analytic function of the initial conditions in the neighborhood of the reference solution.

## Convergence of the Higher Order Solutions

Given the Taylor series expansion of a solution, Eqn. (9), it is not trivial to say what order of solution suffices to represent the local nonlinear motion for a given set of initial deviations. In this section, we discuss a systematic way to find the necessary order of Taylor series that captures the local nonlinear behavior.

The level of nonlinearity (or linearity) of a system's coordinate system can be checked by computing its *nonlinearity index*<sup>5,6</sup>

$$\nu(t, t^o) \triangleq \sup_{k=1, \dots, N} \frac{\|\Phi^k(t, t^o) - \Phi^*(t, t^o)\|_f}{\|\Phi^*(t, t^o)\|_f}, \quad (20)$$

where  $\Phi$ 's are the usual state transition matrices (first order STTs), the superscript  $k$  represents that the solutions are computed along the neighboring trajectories,  $N$  is the number of initial sample points, and  $\|\cdot\|_f$  represents the Frobenius norm. For a given initial error ellipsoid the neighboring trajectories are chosen from the worst-case initial conditions (e.g., boundary points of the 3- $\sigma$  ellipsoid). The nonlinearity index computes the level of maximum linear deviation from the reference trajectory. However, our focus is more on deciding the sufficient order of the higher order solution. For this reason, we apply a similar approach where we instead propagate the deviated trajectory.

For a fixed future time, the idea is to compute the level of nonlinearity that can be approximated by using the STT approach. Let *local nonlinearity convergence rate* defined as follows:

$$\eta^m(t, t^o) \triangleq \sup_{\substack{i=1, \dots, n \\ k=1, \dots, N}} \frac{|\delta \mathbf{x}_i^m(t; \delta \mathbf{x}_k^o, t^o) - \delta \mathbf{x}_i^*(t; \delta \mathbf{x}_k^o, t^o)|}{|\delta \mathbf{x}_i^*(t; \delta \mathbf{x}_k^o, t^o)|}, \quad (21)$$

where  $\delta \mathbf{x}_i^m$  represents a component of the  $m^{\text{th}}$  order STT solution vector and  $\delta \mathbf{x}_k^o$  represents the  $k^{\text{th}}$  sample state vector chosen from the boundary of the initial confidence region (e.g., initial  $N$ - $\sigma$  ellipsoid). Note that the subscripts  $i \in \{1, \dots, n\}$  and  $k \in \{1, \dots, N\}$ , where  $n$  is the system dimension and  $N$  is the number of initial sample points. In other words, we find the state that deviates the most from its reference value over all initial samples and each component of the state vector. The computed value of  $\eta^m$  then tells how well the  $m^{\text{th}}$  order solution can approximate the true nonlinear motion. Using Eqn. (9),  $\eta^m$  can be approximated using the STTs, i.e.,

$$\eta^m(t, t^o) = \sup_{\substack{i=1, \dots, n \\ k=1, \dots, N}} \frac{\left| \left( \sum_{p=1}^m \frac{1}{p!} \Phi_{i, k_1 \dots k_p}^k \delta \mathbf{x}_{k_1}^o \dots \delta \mathbf{x}_{k_p}^o \right) - \delta \mathbf{x}_i^*(t; \delta \mathbf{x}_k^o, t^o) \right|}{|\delta \mathbf{x}_i^*(t; \delta \mathbf{x}_k^o, t^o)|}. \quad (22)$$

As we consider higher order Taylor series and if the series is convergent,  $\eta^m$  will converge to zero, and by increasing the order of solution we can compute the percent difference between the true and STT solutions. Using this notation,  $\eta^m \rightarrow 0$  as  $m \rightarrow \infty$ . As a result, a higher order solution needs to be considered if  $\eta^m > \epsilon$ , where  $\epsilon$  depends on how accurately the user wants to approximate the true nonlinear motion.

## Probability Overview

### Review of the Gaussian Distribution

Consider the spacecraft state vector as a Gaussian random vector (GRV),  $\mathbf{x} \sim \mathcal{N}(\mathbf{m}, \mathbf{P})$ , where  $\mathbf{m}$  is the mean vector and  $\mathbf{P}$  is the covariance matrix. The probability density function for  $\mathbf{x}$  is defined as

$$p(\mathbf{x}) = \frac{1}{\sqrt{(2\pi)^n \det \mathbf{P}}} \exp \left( -\frac{1}{2} (\mathbf{x} - \mathbf{m})^T \mathbf{P}^{-1} (\mathbf{x} - \mathbf{m}) \right). \quad (23)$$

Based on the law of total expectation, the expected value of a function  $\mathbf{g}(\mathbf{x})$  can be computed from

$$E[\mathbf{g}(\mathbf{x})] = \int_{\infty} \mathbf{g}(\boldsymbol{\xi}) p(\boldsymbol{\xi}) d\boldsymbol{\xi}. \quad (24)$$

By definition,

$$\mathbf{m}_i = E[\mathbf{x}_i], \quad (25)$$

$$\mathbf{P}_{ij} = E[\mathbf{x}_i \mathbf{x}_j] - \mathbf{m}_i \mathbf{m}_j. \quad (26)$$

An important property of the Gaussian distribution is that the statistics of GRV can be completely described by the first two moments (i.e.,  $\mathbf{m}$  and  $\mathbf{P}$ ). In other words, the higher moments of  $\mathbf{x}$ , such as  $E[\mathbf{x}_i \mathbf{x}_j \mathbf{x}_k]$  and  $E[\mathbf{x}_i \mathbf{x}_j \mathbf{x}_k \mathbf{x}_l]$ , can all be computed as functions of  $\mathbf{m}$  and  $\mathbf{P}$  and the easiest way to compute them is using the joint characteristic function (JCF).<sup>8</sup> For a Gaussian random vector the JCF is

$$\chi(\mathbf{u}) = E[e^{j\mathbf{u}^T \mathbf{x}}] = \exp\left(j\mathbf{u}^T \mathbf{m} - \frac{1}{2}\mathbf{u}^T \mathbf{P} \mathbf{u}\right), \quad (27)$$

where  $j = \sqrt{-1}$  and the higher moments can be computed as follows:

$$E[\mathbf{x}_{k_1} \mathbf{x}_{k_2} \cdots \mathbf{x}_{k_m}] = j^{-m} \left. \frac{\partial^m \chi(\mathbf{u})}{\partial \mathbf{u}_{k_1} \partial \mathbf{u}_{k_2} \cdots \partial \mathbf{u}_{k_m}} \right|_{\mathbf{u}=\mathbf{0}}. \quad (28)$$

For a nonzero mean GRV,  $\mathbf{x} \sim \mathcal{N}(\mathbf{m}, \mathbf{P})$ , the first four moments become,

$$E[\mathbf{x}_i] = \mathbf{m}_i, \quad (29)$$

$$E[\mathbf{x}_i \mathbf{x}_j] = \mathbf{m}_i \mathbf{m}_j + \mathbf{P}_{ij}, \quad (30)$$

$$E[\mathbf{x}_i \mathbf{x}_j \mathbf{x}_k] = \mathbf{m}_i \mathbf{m}_j \mathbf{m}_k + (\mathbf{m}_i \mathbf{P}_{jk} + \mathbf{m}_j \mathbf{P}_{ik} + \mathbf{m}_k \mathbf{P}_{ij}), \quad (31)$$

$$\begin{aligned} E[\mathbf{x}_i \mathbf{x}_j \mathbf{x}_k \mathbf{x}_l] &= \mathbf{m}_i \mathbf{m}_j \mathbf{m}_k \mathbf{m}_l \\ &+ (\mathbf{m}_i \mathbf{m}_j \mathbf{P}_{kl} + \mathbf{m}_i \mathbf{m}_k \mathbf{P}_{jl} + \mathbf{m}_j \mathbf{m}_k \mathbf{P}_{il} + \mathbf{m}_i \mathbf{m}_l \mathbf{P}_{jk} + \mathbf{m}_j \mathbf{m}_l \mathbf{P}_{ik} + \mathbf{m}_k \mathbf{m}_l \mathbf{P}_{ij}) \\ &+ \mathbf{P}_{ij} \mathbf{P}_{kl} + \mathbf{P}_{ik} \mathbf{P}_{jl} + \mathbf{P}_{il} \mathbf{P}_{jk}. \end{aligned} \quad (32)$$

With the use of symbolic manipulators, computing higher Gaussian moments becomes a simple process.

The Gaussian distribution is used widely for astrodynamics applications due to its simplicity and its invariance under linear operations. When we consider mapping a GRV under nonlinear orbital dynamics, we will see that the Gaussian distribution is no longer preserved since  $\mathbf{x}(t)$  is a nonlinear function of  $\mathbf{x}^o$  in general. However, we can still approximate a non-Gaussian distribution using the first few moments of the variable. This can be checked by comparing the nonlinearly propagated mean and covariance matrix with the Monte-Carlo simulation. The Monte-Carlo mean and covariance matrix are computed based on the following equations:<sup>9</sup>

$$\mathbf{m}_i(t) = \frac{1}{N} \sum_{k=1}^N \mathbf{x}_i^k(t), \quad (33)$$

$$\mathbf{P}_{ij}(t) = \frac{1}{N-1} \sum_{k=1}^N [\mathbf{x}_i^k(t) - \mathbf{m}_i^k(t)] [\mathbf{x}_j^k(t) - \mathbf{m}_j^k(t)], \quad (34)$$

where the superscript  $k$  represents the sample number. Based on the law of large numbers and convergence of the statistics, Eqns. (33) and (34) become the true mean and true covariance matrix as we consider more and more sample trajectories (i.e.,  $N \rightarrow \infty$ ). Precision orbit prediction often relies on Monte-Carlo simulations to predict the future state for nonlinear dynamical situations. However, there are three critical disadvantages when using this approach: (a) the number of sample trajectories may grow quite large to obtain convergence of the statistics, (b) the simulation needs to be repeated for different initial distributions, and (c) it does not provide an analytic work frame. These problems make the Monte-Carlo simulation computationally quite intensive and difficult to interpret. In the next section, we derive a way to avoid these problems by incorporating STT solutions when solving for the mean and covariance matrix at a future time.

## The Fokker-Planck Equation (The Forward Kolmogorov Equation)

Most orbital dynamics problems can be written using the Itô stochastic differential equation,

$$d\mathbf{x}(t) = \mathbf{f}(\mathbf{x}(t), t)dt + \mathbf{G}(\mathbf{x}(t), t)d\boldsymbol{\beta}(t), \quad (35)$$

where  $\mathbf{G}$  is an  $n$ -by- $s$  matrix characterizing the diffusion, i.e.,

$$E[d\boldsymbol{\beta}(t)d\boldsymbol{\beta}^T(t)] = \mathbf{Q}(t)dt, \quad (36)$$

$$E[(\boldsymbol{\beta}(t_2) - \boldsymbol{\beta}(t_1))(\boldsymbol{\beta}(t_2) - \boldsymbol{\beta}(t_1))^T] = \int_{t_1}^{t_2} \mathbf{Q}(t)dt. \quad (37)$$

As an example, the diffusion vector  $\boldsymbol{\beta}$  can be modeled as stochastic acceleration or process noise in case of the spacecraft orbit determination process. The solution to this stochastic differential equation is

$$\mathbf{x}(t) = \mathbf{x}^o + \int_{t^o}^t \mathbf{f}(\mathbf{x}(\tau), \tau)d\tau + \int_{t^o}^t \mathbf{G}(\mathbf{x}(\tau), \tau)d\boldsymbol{\beta}(\tau). \quad (38)$$

Systems with deterministic inputs can be simply rewritten by including them in the state vector.

Now let  $p(\mathbf{x}, t)$  be the probability density function of the stochastic process  $\mathbf{x}(t)$ . Given a system satisfying the Itô stochastic differential equation, the time evolution of the pdf must satisfy the Forward Kolmogorov equation (also known as the Fokker-Planck equation):<sup>4, 10, 11</sup>

$$\begin{aligned} \frac{\partial p(\mathbf{x}, t)}{\partial t} = & - \sum_{i=1}^n \frac{\partial}{\partial \mathbf{x}_i} [p(\mathbf{x}, t)\mathbf{f}_i(\mathbf{x}, t)] \\ & + \frac{1}{2} \sum_{i=1}^n \sum_{j=1}^n \frac{\partial^2}{\partial \mathbf{x}_i \partial \mathbf{x}_j} \left[ p(\mathbf{x}, t)(\mathbf{G}(\mathbf{x}, t)\mathbf{Q}(t)\mathbf{G}^T(\mathbf{x}, t))_{ij} \right], \end{aligned} \quad (39)$$

where the subscript  $i$  represents the  $i^{\text{th}}$  components of a vector and the index ' $ij$ ' represents the  $(i, j)$  component of a matrix. In the following we will consider a system without diffusion terms, resulting the simplified form of the equations

$$\frac{\partial p(\mathbf{x}, t)}{\partial t} = - \sum_{i=1}^n \frac{\partial}{\partial \mathbf{x}_i} [p(\mathbf{x}, t)\mathbf{f}_i(\mathbf{x}, t)]. \quad (40)$$

### Integral Invariance of Probability

Consider a dynamical system  $\mathbf{f}(\mathbf{x}, t)$  and let  $I$  be an integral of a vector field  $M(\mathbf{x}, t)$  over some volume  $\mathcal{V}$

$$I = \int_{\mathcal{V}} M(\mathbf{x}, t)d\mathbf{x}. \quad (41)$$

The integral  $I$  is called an integral invariant if its total time derivative is constant (i.e.,  $dI/dt = 0$ ). The sufficient condition for integral invariance is<sup>12</sup>

$$\frac{\partial M(\mathbf{x}, t)}{\partial t} = - \sum_{i=1}^n \frac{\partial}{\partial \mathbf{x}_i} [M(\mathbf{x}, t)\mathbf{f}_i(\mathbf{x}, t)], \quad (42)$$

and we note that this is identical to the Fokker-Planck equations without diffusion terms. The probability of the state in some phase volume  $\mathcal{B}$  can be computed by integrating the pdf

$$Pr(\mathbf{x} \in \mathcal{B}) = \int_{\mathcal{B}} p(\mathbf{x}, t)d\mathbf{x}. \quad (43)$$

We have that  $p(\mathbf{x}, t)$  satisfies the Fokker-Planck equation of a system with no diffusion terms, Eqn.(40), and that this equation is equivalent to the sufficiency condition for the probability to be an integral invariant. Hence, the probability of *any* dynamical system with no diffusion term is an integral invariant.<sup>13</sup> This result has been discussed by Scheeres *et. al*<sup>14</sup> and combined with Gromov's Non-Squeezing Theory to derive a new set of constraints that exist for orbit uncertainty propagation.

## On the Relation of the Phase Volume and Probability

Suppose we are given an initial  $N$ - $\sigma$  ellipsoid,  $\mathcal{B}_o$ , of the initial state  $\mathbf{x}^o$ . As the probability of a deterministic system is an integral invariant,  $Pr(\mathbf{x} \in \mathcal{B})$  should remain unchanged, which indicates that the propagated  $\mathcal{B}$  is an  $N$ - $\sigma$  *surface* (Note that the name surface is given because its shape is no longer ellipsoidal since the system dynamics are nonlinear in general). This implies that the confidence region of the current state can be defined by nonlinearly mapping the initial phase volume ( $\mathcal{B}_o$ ). This approach is, however, a computationally intensive process since hundreds, even thousands, points from the surface of  $\mathcal{B}_o$  must be integrated using the true nonlinear dynamics. For this reason, we usually work with the simple linear model at a penalty of ignoring the higher order effects. However, once we have the time solution of the STTs, computing the phase volume incorporating the higher order effects becomes a simple algebraic manipulation, which provides a more accurate solution than the linear case. Considering a Hamiltonian (or Lagrangian) system and the uniqueness of solutions, the outer boundary points of an initial phase volume must map to the outer boundary points of the phase volume computed at a later time. Hence we only need to analyze the behavior of the surface of this  $n$ -dimensional object. After the outer boundary points of  $\mathcal{B}_o$  are integrated forward in time, they can be projected onto the position and velocity planes to compute the maximum deviations with respect to the reference trajectory. We note that finding the maximum distance from the center of the phase volume gives the region of confidence which the current state has the same probability as the initial state.

## Solution of the Fokker-Planck Equation for a Deterministic Hamiltonian System

Consider a Hamiltonian,  $H(\mathbf{q}, \mathbf{p}, t)$ , which is a function of an  $n$ -dimensional generalized coordinate  $\mathbf{q}$  and  $n$ -dimensional generalized momentum  $\mathbf{p}$ , hence the system is  $2n$  dimensional. The dynamics equations can be written as

$$\dot{\mathbf{x}}(t) = \mathbf{J}H_{\mathbf{x}}^T, \quad (44)$$

where  $\mathbf{x} = [\mathbf{q}^T \ \mathbf{p}^T]^T$ ,  $H_{\mathbf{x}}$  is the row-wise partial derivative of  $H$  with respect to  $\mathbf{x}$ , and  $\mathbf{J}$  is the symplectic matrix

$$\mathbf{J} = \begin{bmatrix} \mathbf{0} & \mathbf{I} \\ -\mathbf{I} & \mathbf{0} \end{bmatrix}. \quad (45)$$

Both the identity matrices  $\mathbf{I}$  and the zero matrices  $\mathbf{0}$  are  $n \times n$ .

Assuming no diffusion in the dynamics (e.g., no stochastic accelerations), the Fokker-Planck equation for the pdf, Eqn.(39), simplifies to

$$\frac{\partial p(\mathbf{x}, t)}{\partial t} = - \left[ \frac{p(\mathbf{x}, t)}{\partial \mathbf{x}} \dot{\mathbf{x}} + p(\mathbf{x}, t) tr(\mathbf{J}H_{\mathbf{xx}}^T) \right], \quad (46)$$

where  $tr(\cdot)$  represents the trace of a matrix. The second term in the right-hand-side of the above equation vanishes since

$$tr(\mathbf{J}H_{\mathbf{xx}}^T) = tr \begin{bmatrix} H_{\mathbf{pq}} & H_{\mathbf{pp}} \\ -H_{\mathbf{qp}} & -H_{\mathbf{qq}} \end{bmatrix} = 0, \quad (47)$$

and reduces the Fokker-Planck equation to

$$\frac{dp(\mathbf{x}, t)}{dt} = 0. \quad (48)$$

This result is generally true for any system derived from a single potential, and thus, most of the orbital motion represented in Lagrangian form are also satisfied (e.g., Hill 3-body problem, Restricted 3-body problem, etc.). This time invariance, in conjunction with Liouville's Theorem, provides another proof that the probability over some volume  $\mathcal{B}$  (Eqn. 43) is indeed an integral invariant.

Consider  $\mathbf{x}(t) = \phi(t; \mathbf{x}^o, t^o)$  to be the solution flow. From the fundamental theorem of calculus and integral invariance we have

$$Pr(\mathbf{x} \in \mathcal{B}) = \int_{\mathcal{B}} p(\mathbf{x}, t) d\mathbf{x}, \quad (49)$$

$$= \int_{\mathcal{B}_o} p(\phi(t; \mathbf{x}^o, t^o), t) \left| \frac{\partial \mathbf{x}}{\partial \mathbf{x}^o} \right| d\mathbf{x}^o, \quad (50)$$

$$= \int_{\mathcal{B}_o} p(\mathbf{x}^o, t^o) d\mathbf{x}^o, \quad (51)$$

which gives

$$p(\phi(t; \mathbf{x}^o, t^o), t) = p(\mathbf{x}^o, t^o) \left| \frac{\partial \mathbf{x}}{\partial \mathbf{x}^o} \right|^{-1}, \quad (52)$$

where  $|\cdot|$  represents the determinant. For a Hamiltonian system the mapping from  $\mathbf{x}^o$  to  $\mathbf{x}$  is a canonical transformation, and thus,  $|\partial \mathbf{x} / \partial \mathbf{x}^o| = 1$  for all  $t$  according to Liouville's theorem. Hence, the pdf must satisfy

$$p(\phi(t; \mathbf{x}^o, t^o), t) = p(\mathbf{x}^o, t^o), \quad (53)$$

or

$$p(\mathbf{x}, t) = p(\psi(t, \mathbf{x}; t^o), t^o). \quad (54)$$

In other words, the current state pdf can be characterized by the initial pdf, and vice versa. This means that if the solution is known as a function of initial conditions (i.e., is integrated) and the pdf is known at any one time, it can be found for all time. This result is usually assumed in present-day orbit determination process without discussing in details. This is, however, an important property that arises from the structure of the Hamiltonian dynamics. We address implications of this result in a later section of this paper.

## Solution of the Fokker-Planck Equation for a Hamiltonian System with a Gaussian Boundary Condition

Let's consider a special case of practical interest. Suppose our system is modeled using the Hamiltonian dynamics (n.b., the result can be generalized for the Lagrangian systems derived from a single potential) and the initial state can be represented as a GRV with mean  $\mathbf{m}^o = \mathbf{m}(t^o)$  and covariance matrix  $\mathbf{P}^o = \mathbf{P}(t^o)$ , which are *constants*, so that

$$p(\mathbf{x}^o, t^o) = \frac{1}{\sqrt{(2\pi)^{2n} \det \mathbf{P}^o}} \exp \left\{ -\frac{1}{2} (\mathbf{x}^o - \mathbf{m}^o)^T \boldsymbol{\Lambda}^o (\mathbf{x}^o - \mathbf{m}^o) \right\}, \quad (55)$$

where  $\boldsymbol{\Lambda}^o = \mathbf{P}(t^o)^{-1}$ . Recall that the Hamiltonian systems have dimension  $2n$ . Using Eqn. (54), the current state pdf can be stated as

$$p(\mathbf{x}, t) = \frac{1}{\sqrt{(2\pi)^{2n} \det \mathbf{P}^o}} \exp \left\{ -\frac{1}{2} (\psi(t, \mathbf{x}; t^o) - \mathbf{m}^o)^T \boldsymbol{\Lambda}^o (\psi(t, \mathbf{x}; t^o) - \mathbf{m}^o) \right\}. \quad (56)$$

It is easy to show that Eqn. (56) satisfies to be a valid pdf:

$$\int_{\infty} p(\mathbf{x}, t) d\mathbf{x} = \int_{\infty} p(\psi(t, \mathbf{x}; t^o), t^o) d\mathbf{x}, \quad (57)$$

$$= \int_{\infty} p(\mathbf{x}^o, t^o) \left| \frac{\partial \mathbf{x}}{\partial \mathbf{x}^o} \right| d\mathbf{x}^o, \quad (58)$$

$$= 1, \quad (59)$$

where we apply the integral invariance of the pdf and symplectic property of the Hamiltonian system (i.e.,  $|\partial\mathbf{x}/\partial\mathbf{x}^o| = 1$ ). To prove that this is a valid solution we only need to show that  $dp/dt = 0$ . Note that

$$\frac{dp(\mathbf{x}, t)}{dt} = \frac{dp(\psi(t, \mathbf{x}; t^o), t^o)}{dt} = \frac{\partial p}{\partial \psi} \frac{d\psi}{dt}. \quad (60)$$

However  $\psi(t, \mathbf{x}; t^o) = \mathbf{x}^o$  are integrals of motion of our system,<sup>12</sup> and hence, their total time derivative is zero. This derivation is particularly of interest since, as we will see later, it provides evolution of the current state statistics as functions of the initial state and its statistics. An interesting observation that can be made from Eqn. (56) is that the peak of the pdf is always located at the propagated initial mean according to the deterministic map (i.e.,  $\mathbf{x} = \phi(t; \mathbf{m}^o, t^o)$ ); however, the solution flow is nonlinear in general, and thus, the current state mean vector is no longer located at the peak of the distribution. It is apparent from Eqn. (56) that once the state flow  $\phi(t)$  can be represented including the higher order effects and an analytic expression is obtained as a function of the initial state, the statistical moments of the current state can be obtained that are, by definition, more accurate predictions of the propagated statistics than the linear theory. Obtaining an analytic framework of the statistics propagation is discussed in the next section.

## Nonlinear Mapping of the Gaussian Distribution

Consider solving for the mean by integrating the pdf. Applying the results from Eqns. (53) and (54) we have the following four equivalent expressions for the propagated mean:

$$E[\mathbf{x}(t)] = \int_{-\infty}^{\infty} \mathbf{x}(t) p(\mathbf{x}, t) d\mathbf{x}, \quad (61)$$

$$= \int_{-\infty}^{\infty} \phi(t; \mathbf{x}^o, t^o) p(\mathbf{x}^o, t^o) d\mathbf{x}^o, \quad (62)$$

$$= \int_{-\infty}^{\infty} \phi(t; \mathbf{x}^o, t^o) p(\phi(t; \mathbf{x}^o, t^o), t) d\mathbf{x}^o, \quad (63)$$

$$= \int_{-\infty}^{\infty} \mathbf{x}(t) p(\psi(t, \mathbf{x}; t^o), t^o) d\mathbf{x}. \quad (64)$$

We observe that Eqn. (62) is suitable for propagation of the state uncertainties using the STT formulation.

Consider the Gaussian boundary condition for the pdf (Eqn. 55). Assuming nonzero mean for the deviated initial state, the pdf for the initially deviated state,  $\delta\mathbf{x}^o$  can be obtained via a linear transformation,  $\mathbf{x}^o = \delta\mathbf{x}^o + \mathbf{m}^o - \delta\mathbf{m}^o$ , where  $\mathbf{m}^o$  is the initial mean and  $\delta\mathbf{m}^o$  is the initial mean of the deviation. We note that these variables are constants. Applying the change of variable to the pdf yields

$$p(\delta\mathbf{x}^o, t^o) = \frac{1}{\sqrt{(2\pi)^n \det \mathbf{P}^o}} \exp \left\{ -\frac{1}{2} (\delta\mathbf{x}^o - \delta\mathbf{m}^o)^T \mathbf{\Lambda}^o (\delta\mathbf{x}^o - \delta\mathbf{m}^o) \right\}. \quad (65)$$

Since the expectation of the nominal trajectory does not change by definition, it is easier to instead analyze the statistics of the deviated state. Using the STT notation, the current state deviated mean and covariance matrix can be stated as follows:

$$\delta\mathbf{m}_i(t) = \sum_{p=1}^m \frac{1}{p!} \Phi_{i, k_1 \dots k_p} E \left[ \delta\mathbf{x}_{k_1}^o \dots \delta\mathbf{x}_{k_p}^o \right], \quad (66)$$

$$\begin{aligned} \mathbf{P}_{ij}(t) &= \left( \sum_{p=1}^m \sum_{q=1}^m \frac{1}{p!q!} \Phi_{i, k_1 \dots k_p} \Phi_{j, l_1 \dots l_q} E \left[ \delta\mathbf{x}_{k_1}^o \dots \delta\mathbf{x}_{k_p}^o \delta\mathbf{x}_{l_1}^o \dots \delta\mathbf{x}_{l_q}^o \right] \right) \\ &\quad - \delta\mathbf{m}_i(t) \delta\mathbf{m}_j(t), \end{aligned} \quad (67)$$

where  $\{k_j, l_j\} \in \{1, \dots, n\}$ . Note that  $m = 1$  gives the ordinary first-order covariance propagation,<sup>13</sup> i.e.,

$$\delta\mathbf{m}(t) = \mathbf{\Phi} \delta\mathbf{m}^o, \quad (68)$$

$$\mathbf{P}(t) = \mathbf{\Phi} \mathbf{P}^o \mathbf{\Phi}^T - \delta\mathbf{m} \delta\mathbf{m}^T, \quad (69)$$

where  $\Phi$  is the usual state transition matrix and linearly maps the deviation from  $t^o$  to  $t$ . For the cases where  $m > 1$  it is apparent from Eqn. (67) that we need to compute  $2m^{\text{th}}$ -order Gaussian moments, which is, however, a one time operation since we only need to compute the moments of the initial GRV using Eqn. (27). The mean and covariance matrix can thus be obtained as functions of time once we have the time solution of STTs and initial first two moments. This results in the computation of the mean and the covariance matrix to be an algebraic operation. If we consider a zero initial mean, all the odd moments of the initial conditions vanish, which is a property of the Gaussian distribution, and the above equations simplify a great deal. Moreover, it is clear from Eqn. (66) that the mean will not be zero indicating that the mean deviates from the reference trajectory, whereas the linear analysis assumes that the mean is the reference trajectory. As an example, for  $m = 2$  case with zero initial mean, the mean and covariance matrix become functions of the initial covariance matrix  $\mathbf{P}^o$ , i.e.,

$$\delta \mathbf{m}_i(t) = \frac{1}{2} \Phi_{i,ab} \mathbf{P}_{ab}^o, \quad (70)$$

$$\begin{aligned} \mathbf{P}_{ij}(t) &= \Phi_{i,a} \Phi_{j,\alpha} \mathbf{P}_{a\alpha}^o - \delta \mathbf{m}_i \delta \mathbf{m}_j \\ &+ \frac{1}{4} \Phi_{i,ab} \Phi_{j,\alpha\beta} [\mathbf{P}_{ab}^o \mathbf{P}_{\alpha\beta}^o + \mathbf{P}_{a\alpha}^o \mathbf{P}_{b\beta}^o + \mathbf{P}_{a\beta}^o \mathbf{P}_{b\alpha}^o]. \end{aligned} \quad (71)$$

Considering this fact, updating future measurements with respect to the mean trajectory will provide more accurate information about the true trajectory, and thus, faster convergence of the estimation process may be obtained. This also provides more precise predictions of where the true trajectory is.

## Applications of the STT Propagated Statistics

In this section we discuss several spacecraft applications where the nonlinear uncertainty propagation can be utilized. We first introduce the concept of statistically correct trajectory targeting where we discuss how to incorporate statistical information into the trajectory design. We then extend this idea and present the nonlinear statistical targeting by computing the correction maneuver that gives the statistically correct target position at a desired time.

### The Concept of Statistically Correct Trajectory

Conventional mission design usually relies on the deterministic solution of a boundary value problem and no statistical information is taken into account in the design process. The idea of statistically correct trajectory is to compensate this deterministic trajectory by incorporating the statistical information. Figure 1 shows the concept of the statistically correct trajectory. Suppose the trajectory  $\mathbf{x}(t)$  deterministically gives the desired target state at  $t^f$  (i.e.,  $\mathbf{x}(t^f) = \phi(t^f; \mathbf{x}^o, t^o) = \mathbf{x}^f$ ). However, in practice,  $\mathbf{x}^o$  is uncertain (e.g.,  $\mathbf{x}^o \sim \mathcal{N}(\mathbf{m}^o, \mathbf{P}^o)$ ), and therefore, the mean trajectory,  $\mathbf{m}^f = E[\phi(t^f; \mathbf{x}^o, t^o)]$ , deviates from the target state. In other words, the most likely state at time  $t^f$  is not  $\mathbf{x}^f$ , but rather  $E[\phi(t^f; \mathbf{x}^o, t^o)] = \mathbf{m}^f \neq \mathbf{x}^f$  according to probability theory and  $\delta \mathbf{m}^f = \mathbf{m}^f - \mathbf{x}^f$  is not zero. Given this fact and assuming the spacecraft is initially located at the initial nominal orbit, there exist initial neighboring trajectories  $\mathbf{x}^o + \delta \mathbf{m}^o$  such that their initial states are offset from the reference state, but their deviated trajectory reach the desired final state at some time  $t^k$ . Mathematically speaking, we want to find  $\delta \mathbf{m}^o$  such that  $E[\phi(t^k; \mathbf{x}^o + \delta \mathbf{m}^o, t^o)] = \mathbf{x}^f$ . In general we note that time (i.e.,  $t^k$  does not have to be  $t^f$ ) is a free parameter in this problem, and hence, we solve to minimize the magnitude of  $\delta \mathbf{m}(t^k)$  with respect to the final state. This, however, is a rather counter intuitive method since we suggest that we aim for a different state rather than the target. We call this trajectory the *statistically correct trajectory* and the goal is to find  $\delta \mathbf{m}^o$  satisfying  $\delta \mathbf{m}(t^k) = E[\phi(t^k; \mathbf{x}^o + \delta \mathbf{m}^o, t^o)] - \mathbf{x}^f = 0$ .

For an initial Gaussian boundary condition, the deviated mean can be represented as a power series in the deviated initial mean  $\delta \mathbf{m}^o$  and covariance  $\mathbf{P}^o$  using Eqn. (66). As an

example, the 3<sup>rd</sup> order STT-propagated mean can be analytically stated as

$$\delta \mathbf{m}_i(t^k) = \sum_{p=1}^3 \frac{1}{p!} \Phi_{i,k_1 \dots k_p} E \left[ \delta \mathbf{x}_{k_1}^o \cdots \delta \mathbf{x}_{k_p}^o \right], \quad (72)$$

$$\begin{aligned} &= \Phi_{i,a} \delta \mathbf{m}_a^o + \frac{1}{2!} \Phi_{i,ab} (\delta \mathbf{m}_a^o \delta \mathbf{m}_b^o + \mathbf{P}_{ab}^o) \\ &+ \frac{1}{3!} \Phi_{i,abc} (\delta \mathbf{m}_a^o \delta \mathbf{m}_b^o \delta \mathbf{m}_c^o + \delta \mathbf{m}_a^o \mathbf{P}_{bc}^o + \delta \mathbf{m}_b^o \mathbf{P}_{ac}^o + \delta \mathbf{m}_c^o \mathbf{P}_{ab}^o). \end{aligned} \quad (73)$$

Applying this analytic expression, the solution can be found via an iterative process such as the Newton's method, i.e.,

$$\delta \mathbf{m}(t^o)^{i+1} = \delta \mathbf{m}(t^o)^i - \left. \left( \frac{\partial(\delta \mathbf{m}(t^k))}{\partial(\delta \mathbf{m}(t^o))} \right)^{-1} \right|_{\delta \mathbf{m} = \delta \mathbf{m}^i} \cdot \delta \mathbf{m}(t^k; \delta \mathbf{m}(t^o)^i), \quad (74)$$

with the initial guess of

$$\delta \mathbf{m}(t^o)^i = \Phi^{-1} \delta \mathbf{m}(t^f), \quad (75)$$

and carry out the iteration until  $\delta \mathbf{m}(t^o)^{i+1}$  is sufficiently small. We note that if we fix the final time (i.e,  $t^k = t^f$ ), the solution exists for the cases with sufficiently small initial uncertainties. After solving for  $\delta \mathbf{m}^o$ , the statistically correct initial condition is  $\mathbf{x}^o + \delta \mathbf{m}^o$  for the given initial covariance matrix.

## Nonlinear Statistical Targeting

As an extension of the statistically correct trajectory, we can design a nonlinear statistical correction maneuver using the similar approach. In this paper, we focus on position targeting based on a single impulsive maneuver; however, the result can be generalized to target the full state with two or more maneuvers. Figure 2 illustrates the concept of the nonlinear statistical targeting method. In particular, let  $\mathbf{r}^f = \mathbf{r}(t^f)$  be the fixed target position and  $\mathbf{v}^f = \mathbf{v}(t^f)$  be the velocity vector which can vary. We want to design a maneuver  $V_k$  such that  $E[\phi_r(t^f; \mathbf{r}^k + \delta \mathbf{m}_r^k, \mathbf{v}^k + \delta \mathbf{m}_v^k + \Delta V_k, t^k)] = \mathbf{r}^f$ , where  $\phi_r$  represents the solution flow of the position components. In other words, we solve for  $\Delta V_k$  such that  $\delta \mathbf{m}_r(t^f) = 0$ , which can be stated analytically similar to Eqn. (66). We note that  $i \in \{1, \dots, n/2\}$  since only the position mean is needed to be solved.

When we consider the first order STT (i.e., conventional linear targeting) we are solving for  $\Delta V_k$  that satisfies,

$$\delta \mathbf{m}_r(t^f) = \Phi_{rr}(t^f, t^k) \delta \mathbf{m}_r(t^k) + \Phi_{rv}(t^f, t^k) (\delta \mathbf{m}_v(t^k) + \Delta V_k) = 0, \quad (76)$$

where  $\Phi$ 's are the usual state transition matrices mapping the deviation from  $t^k$  to  $t^f$ . Solving for  $\Delta V_k$  yields the linear correction maneuver

$$\Delta V_k = -\Phi_{rv}^{-1} \Phi_{rr} \delta \mathbf{m}_r(t^k) - \delta \mathbf{m}_v(t^k). \quad (77)$$

With this linear correction, the deviated position is deterministically solved to be zero, (i.e.,  $\delta \mathbf{r}(t^f) = 0$ ). However, we know that the true trajectory will miss the desired target (depending on the associated uncertainties at  $t^k$ , transit period  $t^f - t^k$ , system nonlinearity, etc.) and that this deviation may be significant.

As in the statistically correct trajectory case, the correction maneuver  $\Delta V_k$  can be computed via an iterative process as in the statistically correct trajectory case. Assuming that the deviated mean is computed using the necessary order of the  $m^{\text{th}}$  order STT solution, only one correction maneuver is required to hit the desired target in a statistical sense. In terms of  $\Delta V_k$  cost, the linear targeting method predicts that it is better to perform correction maneuvers in an early stage of the trajectory, since the deviated mean is smaller. This yields a trade-off between the final deviation and the  $\Delta V_k$  cost (i.e., if a maneuver is performed earlier the trajectory deviates more). Using the nonlinear method, we will always achieve (in a statistical sense) zero for the final deviated position mean and later examples show that in most cases there is an optimal location (minimum  $\Delta V_k$ ) to perform the correction maneuver.

## Discussion

Although, in theory, the nonlinear statistical targeting provides a maneuver that is more realistic and accurate than the linear theory, there are practical, as well as fundamental, problems that must be discussed before we present results. First we note that the nonlinear statistical targeting depends on the statistical knowledge about the epoch state whereas the linear correction maneuver is independent of the statistics, and hence, there is only one maneuver (assuming impulsive) to solve for in the linear targeting problem. The statistical part of the linear maneuver is then checked by running the Monte-Carlos runs to ensure that the spacecraft resides in a necessary error bound at the target. This is often carried out based on larger-than-estimated initial uncertainties so that a more conservative distribution can be treated at the target. However, we must keep in mind that the navigation data is the only information we will have about the trajectory and the linear correction completely ignores this information in the design process.

For the nonlinear maneuver, however, the dependency on the navigation data makes the nonlinear targeting more difficult for the maneuver designers since the calibrated initial uncertainties will provide a different maneuver. This is precisely the place where we can make an important, yet distinct, comparison between the two methods. Our study shows that the nonlinearly propagated mean provides a more *conservative* solution than the linear solution. We mean *conservative* by that the resulting projection of the covariance matrix using the nonlinear correction gives a more dispersed uncertainties at the state since the covariance matrix is positively affected (i.e., the covariance matrix is increased) by the deviated mean. Hence, the initial uncertainties do not need to be calibrated to encompass possible additional errors. An obvious question one may ask is, what if the navigation data is perceived to be too accurate, so the uncertainties were doubled (e.g.,  $1\text{-}\sigma$  to  $2\text{-}\sigma$ ), or there are other uncertainty data from different navigation sources. If there is only one initial distribution, we are actually increasing the region of event space to obtain a higher probability by increasing the initial uncertainties. Hence, the covariance matrix should remain unchanged in the maneuver design process. When the uncertainties are increased to check the linear maneuver using the Monte-Carlo simulation, it actually means that a larger initial error ellipsoid is considered to increase the probability, not the covariance matrix. This indicates that both methods are, in a way, utilizing the navigation data, but the nonlinear statistical targeting includes the navigation data in the maneuver design process. If there are initial distributions from different navigation sources, it will be the maneuver designer's decision to choose which navigation data to be used.

If the navigation data is extremely accurate and if the system behaves linearly, both correction maneuvers are essentially the same; however, there are usually significant levels of uncertainties associated at an epoch and two results will be different. Consider an extreme case where the dispersion of the initial uncertainties are very large and the target is sufficiently far from the epoch. By applying the linear correction, we completely ignore the current statistical knowledge about the trajectory, and as a result, we know for sure that the spacecraft will miss the target. This problem is remedied by applying several correction maneuvers along the trajectory as the spacecraft is determined to lie outside the required confidence region. As a comparison, consider applying maneuvers as in the linear case, but instead applying nonlinear maneuvers. A practical importance of the nonlinear method is that the number maneuvers can be reduced when the nonlinear correction is used because the spacecraft will more likely lie within the necessary confidence region for a longer period.

In nonlinear statistical targeting, we instead aim for the deviated mean whereas the linear correction aims for the target on the reference trajectory. From the integral invariance of the probability, it is easy to show that the reference trajectory always depicts the highest value of the probability density function for the initial Gaussian state, and hence, the linear correction maneuver is in a sense the most probable targeting correction. This fact is a theoretically very interesting point. However, the target point is a single event in the probability space, and hence, has a zero probability. On the other hand, the mean is, by definition, the expected value of the deviated state, and hence, is the most likely mapped state for the given initial distribution. It is true that an infinitesimal volume around the reference will have the highest probability, but this probability is negligible when compared

$\eta^m$	Two-Body	Hill Three-Body
$\eta^1$	1.06	3.57
$\eta^2$	0.04	0.29
$\eta^3$	0.007	0.28
$\eta^4$	0.001	0.06

**Table 1 Level of Higher Order Effect**

to the initial phase volume we consider, i.e., an  $N$ - $\sigma$  ellipsoid. To make a clear comparison, we must consider the probability of the entire confidence region. In other words, both the target and mean have zero probabilities in the probability space, but the mean is the most likely final location given the initial phase volume.

## Examples

In this section, we present several examples based on the two-body and Hill three-body body problems. The two-body motion is based on the Earth-to-Moon Hohmann transfer and the Hill three-body model is about the Jupiter-Europa system.

### Two-Body Problem

The governing equations of motion for the planar two-body problem<sup>15</sup> are given as

$$\ddot{x} = -\frac{\mu_{\oplus}}{r^3}x, \quad (78)$$

$$\ddot{y} = -\frac{\mu_{\oplus}}{r^3}y. \quad (79)$$

Figure 3 shows a Hohmann transfer from near Earth (20,000 km) to the Moon (384,400 km). The orbit is propagated for the transfer period ( $\sim 5.24$  days) and the initial statistics are assumed to be zero mean with position uncertainty of 100 km and velocity uncertainty of 0.1 m/s. When computing  $\eta$ , eight sample points corresponding to the eigenvectors of the initial error ellipsoid are considered. Table 1 shows the *local nonlinearity convergence rate*. The result shows that the series is convergent and the second order solution provides superior result than the first order case as predicted by the *local nonlinearity convergence rate*. Figure 4 shows the propagated mean and 1- $\sigma$  ellipsoid plotted with respect to the target state (i.e, apoapsis) where the Monte-Carlo result is based on the ensemble of  $10^6$  sample points. The result shows that the second and higher order solutions provide a far more accurate estimate of the mean and the dispersion of the samples (i.e., projection of the covariance matrix) than the linear (first order) solution.

In this two-body case, we assume that the 3<sup>rd</sup> order STT-solution is considered to be the true Monte-Carlo solution, and thus, the  $\Delta V_k$  computed using the STT method gives the zero deviated position mean. We first solve for the STT solutions of the entire Hohmann transfer ( $t^o$  to  $t^f$ ) and compute the deviated mean at some time  $t^k$ . We then re-solve for the STT solutions from the deviated mean at  $t^k$  to  $t^f$  and find the correction  $\Delta V_k$  using Eqn. (??). There are ways to avoid integrating the STT solutions for each  $t_k$ , such as using the inverse solution of the STTs; however, this is not considered in this study. At every instance of the the deviated mean trajectory, the position and velocity uncertainties are assumed to be 100 km and 0.1 m/s, respectively, which is the same as the initial uncertainties. Figure 5 shows the  $\Delta V_k$  corrections computed using the linear and nonlinear methods as function of the true anomaly applied along the deviated mean trajectory. Both solutions become essentially the same after  $\theta \approx 90$  degrees; indicating small nonlinearity for the later part of the transfer. As expected, the linear solution  $\Delta V_k$  grows as the correction maneuver is made at a later time due to a more deviated mean trajectory. We note that there is an optimal (minimum  $|\Delta V_k|$ ) place to perform a correction maneuver that targets the position mean. Figure 6 shows the deviated position and velocity means at the target. The nonlinear deviated position is not shown since it is zero by definition. When the correction maneuver is made at an early stage of the trajectory using the linear theory, the position mean may deviate quite a bit. For the deviated velocity mean, the difference between the linear and nonlinear solutions is very small.

## Hill Three-Body Problem

The governing equations of motion for the planar Hill three-body problem in non-dimensional form are given as<sup>16</sup>

$$\ddot{x} = 2y - \frac{x}{r^3} + 3x, \quad (80)$$

$$\ddot{y} = -2\dot{x} - \frac{y}{r^3}. \quad (81)$$

The units can be dimensionalized by using the length scale of  $(\mu_E/\omega^2)^{1/3}$  and time scale of  $(1/\omega)$ . The reference trajectory in non-dimensional coordinates is shown in Figure 7, where the final position is located at the periapsis. The initial conditions used are

$$\mathbf{r}(t_o) = [ 0.69010031015662 \quad -0.06716709529872 ], \quad (82)$$

$$\mathbf{v}(t_o) = [ -0.11045639526249 \quad 0.03184084790390 ], \quad (83)$$

which is slight below the  $L_2$  point with Jacobi integral value of -2.15. Moreover, the initial state is assumed to have a zero mean with position error of 10 km and velocity error of 0.1 m/s. The *local nonlinearity convergence rate* given in Table 1 shows that the fourth order solution provides accuracy better than 10 percent error. The level of accuracy can be improved when a different target is considered since the periapsis is the state with a strong nonlinearity. In Figure 8, as in the two-body case, the Monte-Carlo result is based on the  $10^6$  ensemble of initial samples. It is clear that the higher order solution provides a superior result as compared to the linear case. We can see this from the location of the deviated mean and the dispersion of the Monte-Carlo samples.

Similar to the two-body case, the 4<sup>th</sup> order STT-solution is considered to be the true Monte-Carlo solution and we assume the mean trajectory has uncertainties that are the same as the initial state, i.e., 10 km for the position components and 0.1 m/s for the velocity components. Figure 9 shows the  $\Delta V_k$  applied at  $t^k$  that are solved using both the linear and nonlinear methods. The correction maneuvers are plotted as functions time and we observe small nonlinearity approximately from  $t^k \approx 15$  hours. In this case, however,  $\Delta V_k$  fluctuates around  $t^k = 4$  hours in both cases unlike the two-body case. This is due to a sudden change in the velocity direction, and hence, the system nonlinearity is varied. There is also an optimal  $|\Delta V_k|$ , which occurs around  $t^k \approx 15$  hours. Figure 10 shows the deviated position and velocity means. As in the two-body case, when the correction maneuver is made at an early stage of the trajectory using the linear theory, the position mean may deviate noticeably. The overall difference between the linear and nonlinearly computed velocity mean is very small. A high fluctuation in the nonlinearly solved  $\delta \mathbf{m}_v(t^f)$  is due to the higher correction maneuvers in that time frame.

## Discussion

Several important observations can be made from the previous examples. First observation is that the linear (first order) solution captures the semi-major axis of the true covariance plot and the semi-minor axis depends on the deviated mean. Second is that the propagated linear mean (i.e., reference state) lies inside the true covariance projection. As a result the nonlinear (or higher order) uncertainty propagation provides a more conservative estimate of the future statistics. This is important since a more stringent error bound can be computed.

## Conclusion

In this study, we have developed an analytic expression of a nonlinear trajectory solution by solving for the higher state transition tensors that describe the localized nonlinear motion about a nominal trajectory. We then discussed a fundamental property of the uncertainty propagation by proving the integral invariance of the probability density function via solutions of the Fokker-Planck equations for diffusion-less systems. Also presented is the relation between the phase volume and the probability density function since they actually

possess the same statistical information, but are represented in different ways. Applying the nonlinear state propagation and the integral invariance of the probability density function, we have derived an analytic representation of the nonlinear uncertainty propagation and have shown that a sufficient order of STT-approach essentially resembles the Monte-Carlo simulations. This led us to introduce the concept of the statically correct trajectory and its practical application, the nonlinear statistical targeting. The nonlinear statistical targeting allows to utilize the statistical property of the trajectory in the maneuver design process, and thus, provides a statistically more accurate solution. When the initial uncertainties are negligibly small, the nonlinear method essentially becomes the linear solution; however, when there is sufficiently large initial uncertainties the solution gives the most probable maneuver according to the probability theory. The results from the two-body and Hill three-body examples show that there are cases where optimal place perform the maneuver which is not featured by the linear method.

## Acknowledgement

The research described in this paper was sponsored by the JIMO program from Jet Propulsion Laboratory, California Institute of Technology which under contract with the National Aeronautics and Space Administration. The authors would like to thank Jon Sims, John Aiello, Lou D'Amario, Chris Potts, and Mau Wong from the Jet Propulsion Laboratory for their helpful comments and suggestions.

## References

- <sup>1</sup>Battin, R. H., *An Introduction to the Mathematics and Methods of Astrodynamics*, AIAA Education Series, AIAA, revised ed., 1999.
- <sup>2</sup>Montenbruck, O. and Gill, E., *Satellite Orbits*, Springer, 2nd ed., 2001, pp. 257-291.
- <sup>3</sup>Crassidis, J. L. and Junkins, J. L., *Optimal Estimation of Dynamics Systems*, CRC Press LLC, 2004.
- <sup>4</sup>Maybeck, P. S., *Stochastic Models, Estimation, and Control. Vol 2*, Academic Press, 1982.
- <sup>5</sup>Junkins, J., Akella, M., and Alfriend, K., "Non-Gaussian Error Propagation in Orbit Mechanics," *Journal of the Astronautical Sciences*, Vol. 44, No. 4, 1996, pp. 541-563.
- <sup>6</sup>Junkins, J. and Singla, P., "How Nonlinear Is It? A Tutorial on Nonlinearity of Orbit and Attitude Dynamics," *The Journal of the Astronautical Sciences*, Vol. 52, No. 1 and 2, 2004, pp. 7-60.
- <sup>7</sup>Park, R. and Scheeres, D., "Nonlinear Mapping of Gaussian State Covariance and Orbit Uncertainties," *Space Flight Mechanics Meeting*, January, 2005, Copper Mountain, Colorado, AAS 05-170.
- <sup>8</sup>Maybeck, P. S., *Stochastic Models, Estimation, and Control. Vol 1*, Republished by Navtech Book & Software Store, 1994.
- <sup>9</sup>Lass, H. and Gottlieb, P., *Probability and Statistics*, Addison-Wesley, 1971.
- <sup>10</sup>Risken, H., *The Fokker-Planck Equation*, Springer-Verlag, 1984.
- <sup>11</sup>Frank, T., *Nonlinear Fokker-Planck Equations*, Springer-Verlag, 2005.
- <sup>12</sup>Greenwood, D. T., *Classical Dynamics*, Dover Publications, 1997.
- <sup>13</sup>Scheeres, D. J., Han, D., and Hou, Y., "Influence of Unstable Manifolds on Orbit Uncertainty," *Journal of Guidance, Control, and Dynamics*, Vol. 24, 2001, pp. 573-585.
- <sup>14</sup>Scheeres, D., Hsiao, F.-Y., Park, R., Villac, B., and Maruskin, J., "Fundamental Limits on Spacecraft Orbit Uncertainty and Distribution Propagation," *Shuster Symposium*, 2005, AAS 05-471.
- <sup>15</sup>Prussing, J. and Conway, B., *Orbital Mechanics*, Oxford University Press, Inc., New York, 1993.
- <sup>16</sup>Pollard, H., *Celestial Mechanics*, The Mathematical Association of America, 1976.

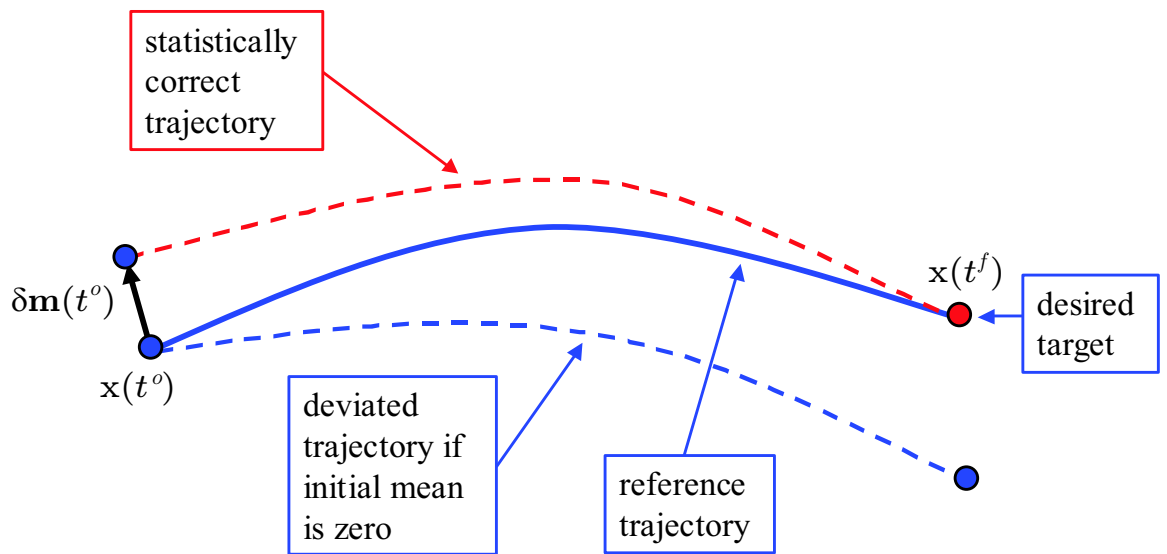


Fig. 1 Illustration of the statistically correction trajectory.

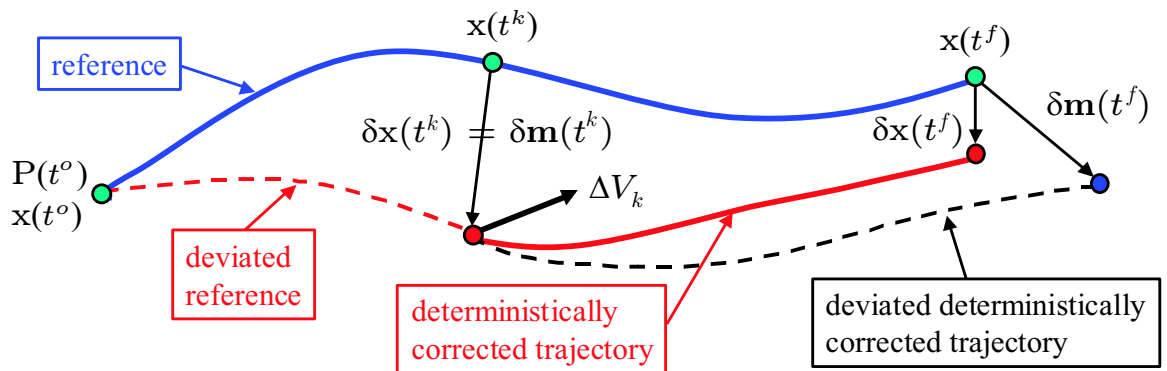


Fig. 2 Illustration of the nonlinear statistical targeting.

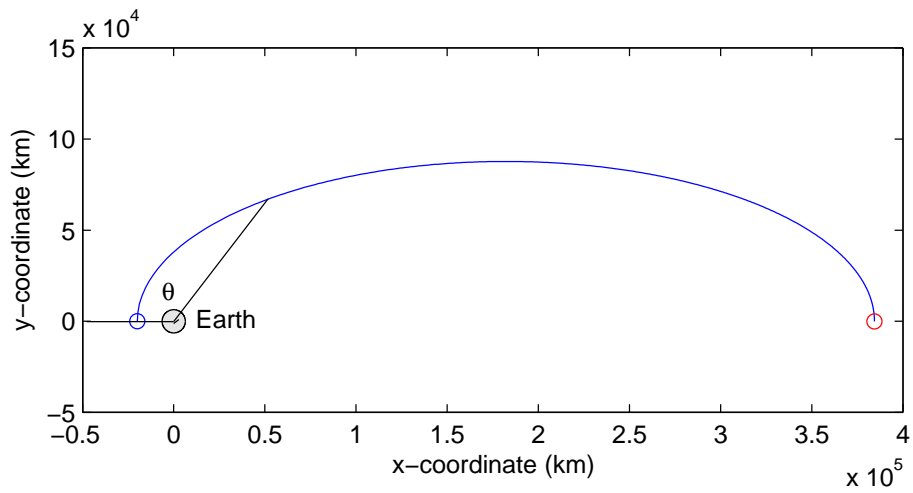


Fig. 3 Two-body Hohmann transfer trajectory.

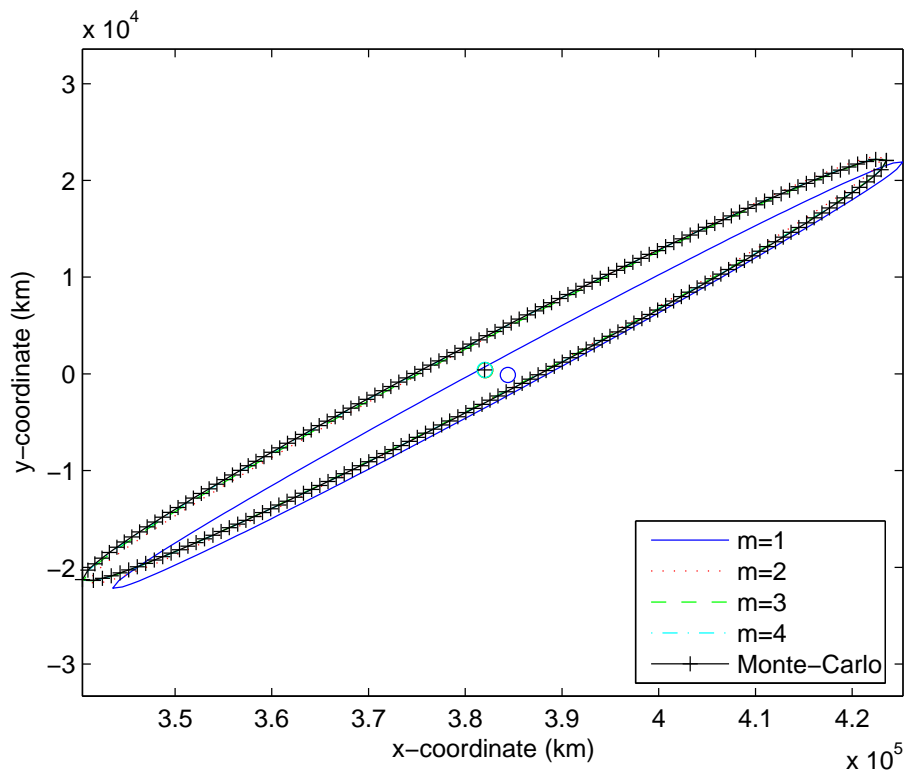


Fig. 4 Comparison of the computed mean and covariance using STT-approach and Monte-Carlo simulations.

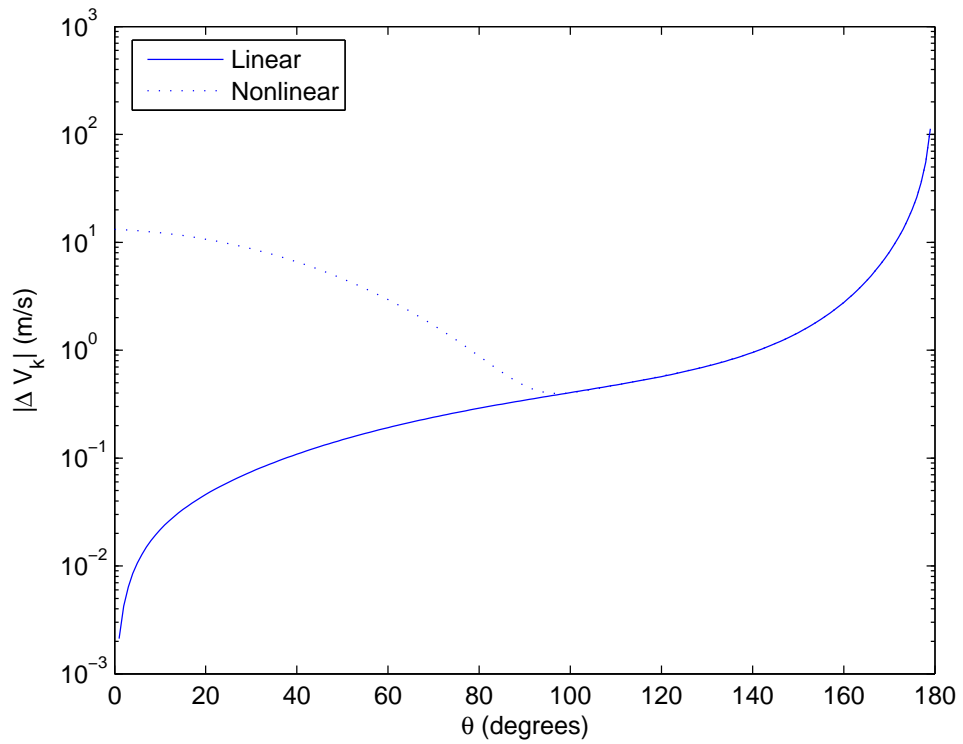


Fig. 5 Computed  $\Delta V_k$  using the linear and nonlinear methods.

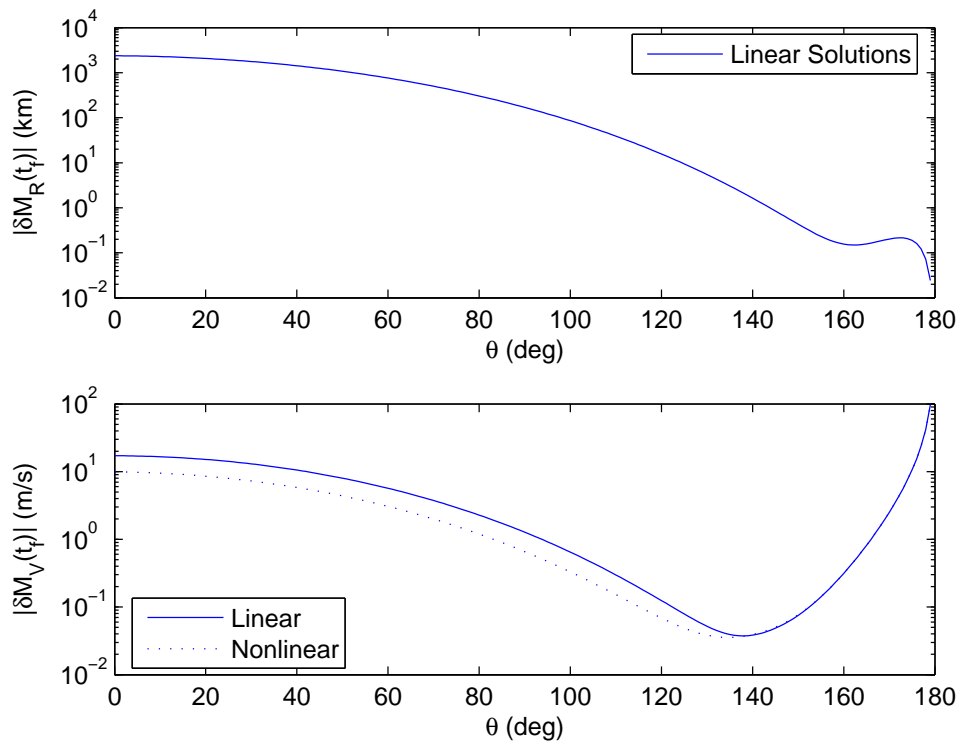


Fig. 6 Deviated position and velocity means at the target.

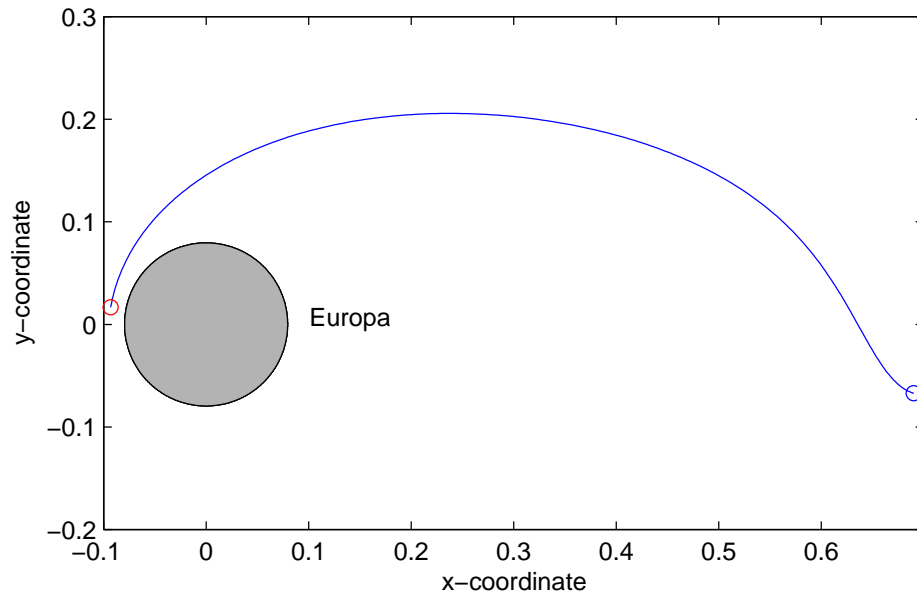


Fig. 7 Hill three-body trajectory.

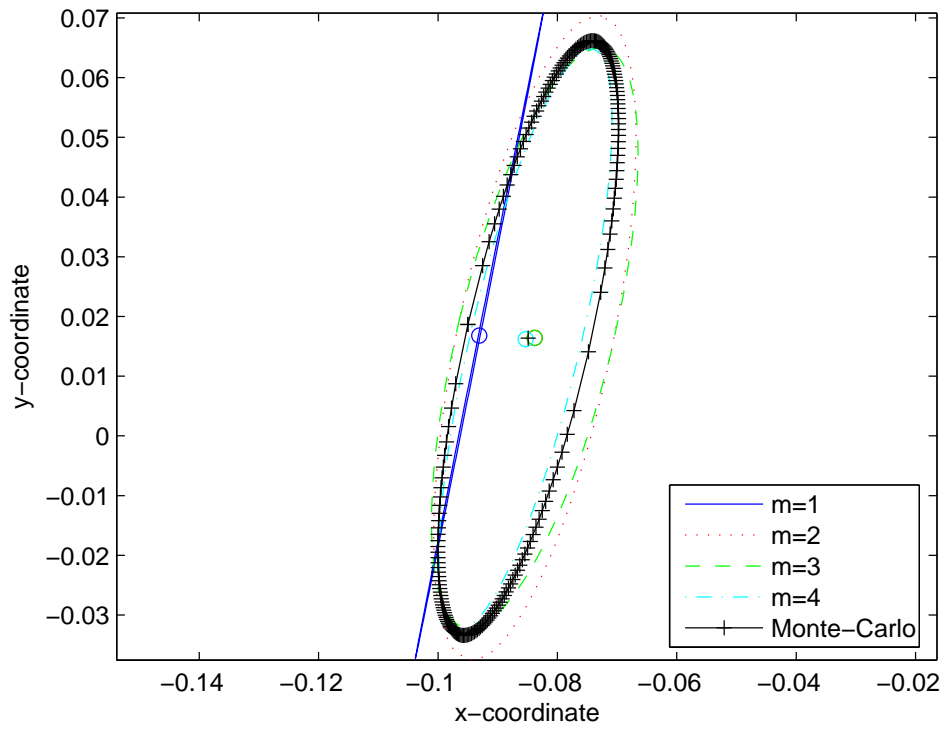


Fig. 8 Comparison of the computed mean and covariance using STT-approach and Monte-Carlo simulations.

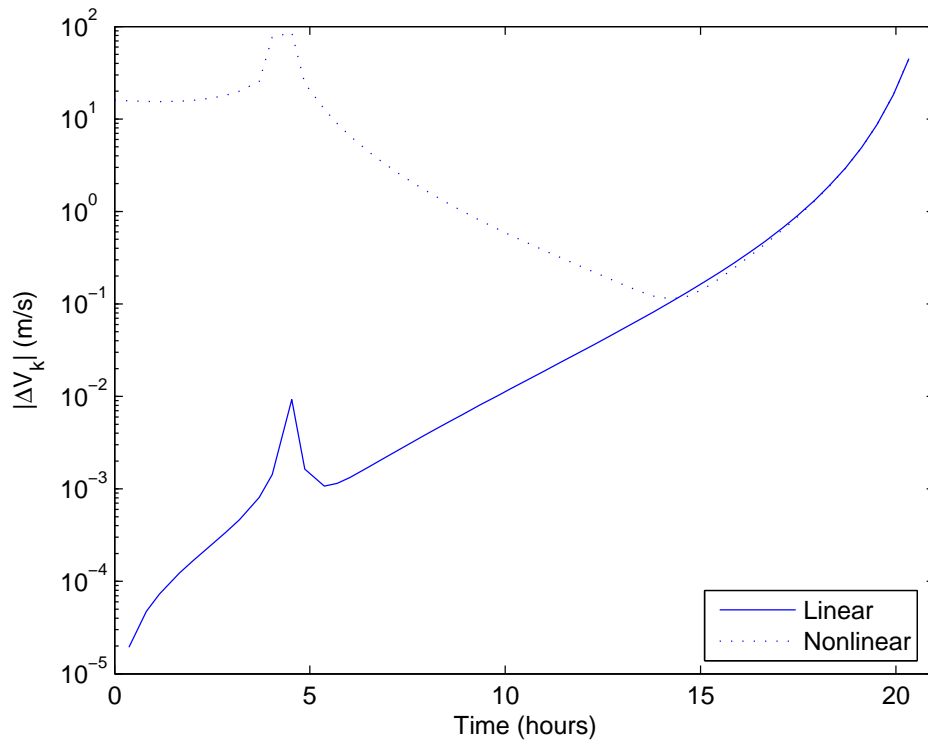


Fig. 9 Computed  $\Delta V_k$  using the linear and nonlinear methods.

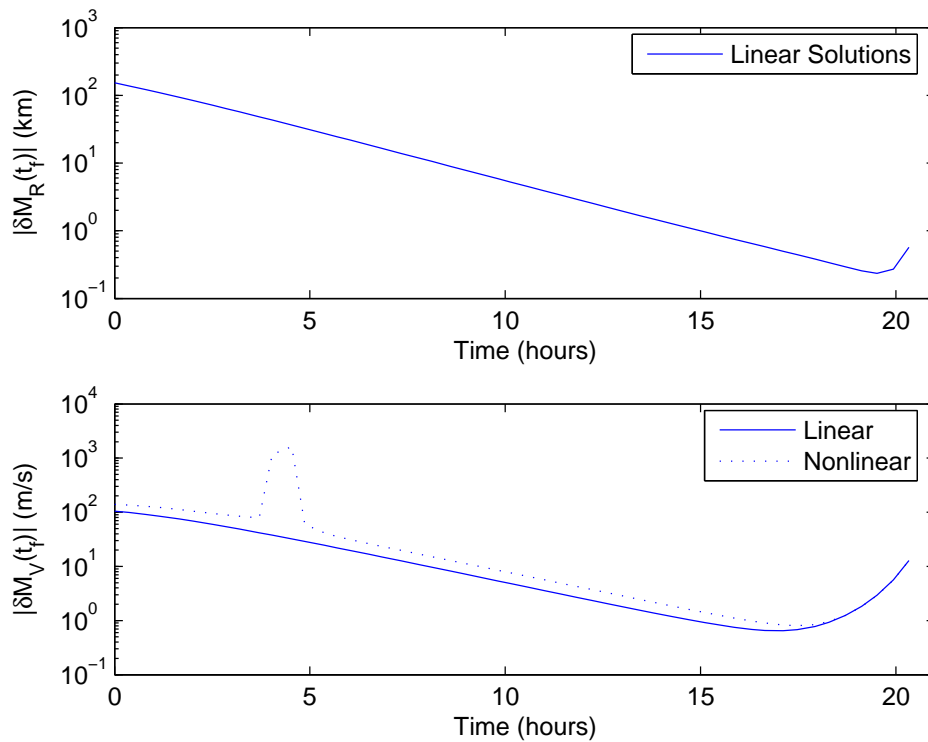


Fig. 10 Deviated position and velocity means at the target.